Supplementary Information

Magnetic, X-ray and Mössbauer studies on Magnetite/Maghemite Core-Shell Nanostructures Fabricated through Aqueous Route.

Srividhya J. Iyengar, Mathew Joy, Chandan Kumar Ghosh, Subhrajyoti Dey, Ravinder K. Kotnala, and Swapankumar Ghosh*

Instrumental characterization

Activation energy for the growth of magnetite crystals during syntheses at different temperatures are shown in eqn (S1).

$$D_{XRD} = k.e^{-\left(\frac{E}{RT}\right)} \quad \text{(S1)}$$

where, D_{XRD} is the crystallite size, R the universal gas constant, T the reaction temperature, E is the activation energy and k is a constant which may depend on the initial value of crystal size.

Particle size (D_{SA}) was also calculated from the BET surface area (S_{SA}) using Eq (S2) with an assumption that all the particles are spherical and unclustered.

$$D_{SA} = \frac{6000}{\rho S_{SA}} \quad \text{(S2)}$$

where ρ=5.18 g.cm^{-3} for magnetite. Size measurements for the magnetite nanoparticles by dynamic light scattering technique and their surface charge was estimated by measuring zeta potentials of their suspensions as a function of pH from 2.8 to 12.0 using a Zetasizer Nano-ZS (Malvern Instruments, Malvern, UK) at 25 °C. Measurements were performed on stable suspensions 1 day after preparation.

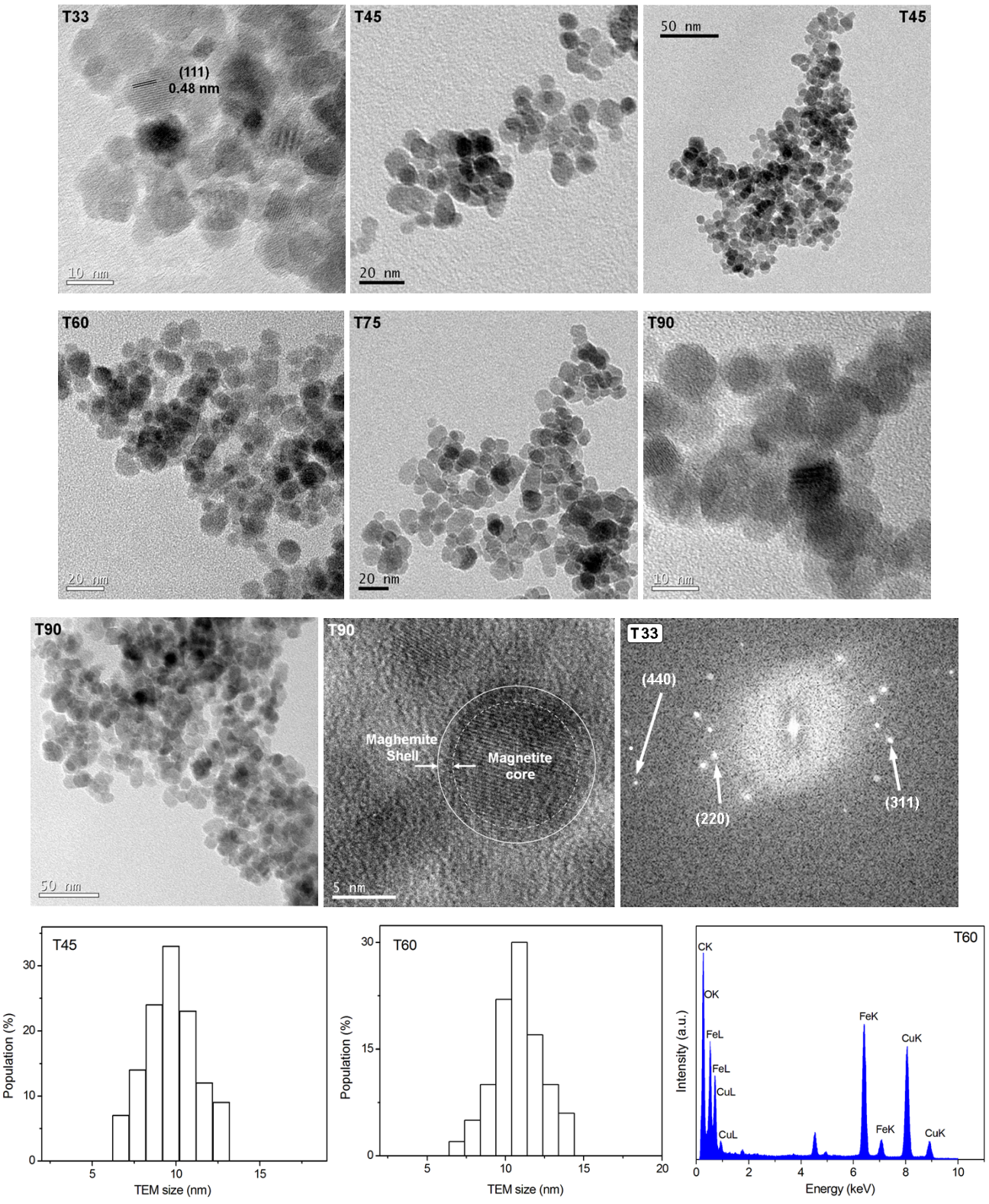

Fig. S1 Additional TEM, micrographs of all Fe_3O_4 samples, confirming the 2D appearance, HRTEM representing magnetite core-maghemite shell, FFT of Fig. 1D, size distributions, and EDAX analysis.

The Williamson-Hall plots of $\beta\cos\theta$ versus $\sin\theta$ for the nanocrystalline magnetite samples using (220), (311), (400), (511) and (440) Bragg reflections and the calculated lattice parameter change 'Δa' as a function of the crystallite sizes, "D" are presented in Fig. S2. This could be due to the presence of magnetically dead layer on the surface of magnetite crystals at higher temperatures.

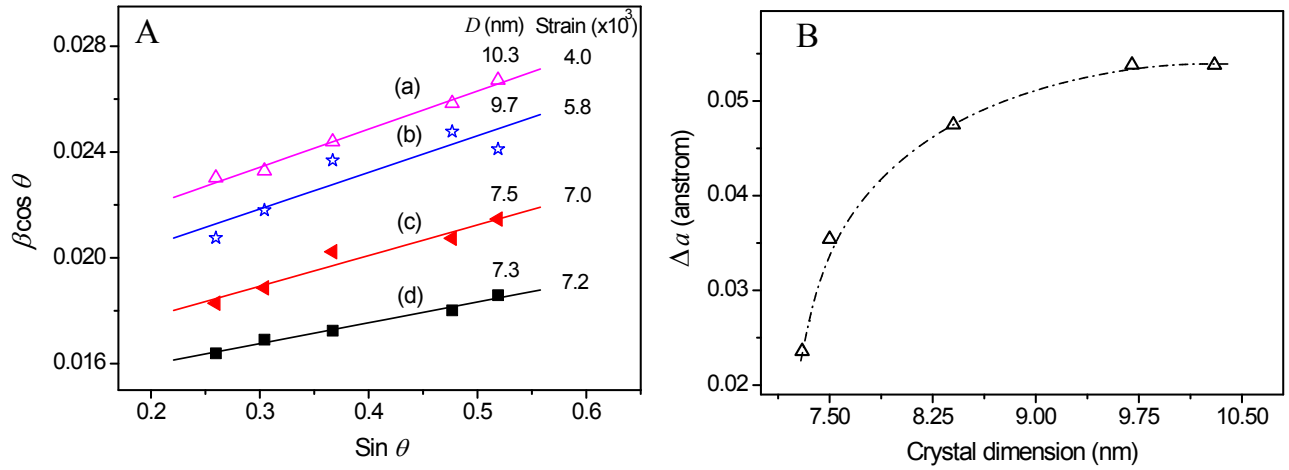

Fig. S2 (A) Williamson-Hall plot of $\beta\cos\theta$ versus $\sin\theta$ for the reasonably well-resolved Bragg lines of Fe_3O_4 nanocrystals (a) T33, (b) T45, (c) T75, and (d) T90 synthesised at different temperatures. The straight lines are the fits to the data. The calculated crystal dimensions and lattice strains evaluated from the linear fits are shown with corresponding data layers. (B) Change in lattice parameter (Δa) calculated from their powder X-ray diffraction patterns (reference JCPDS card No. 19-0629 is used for the calculations).

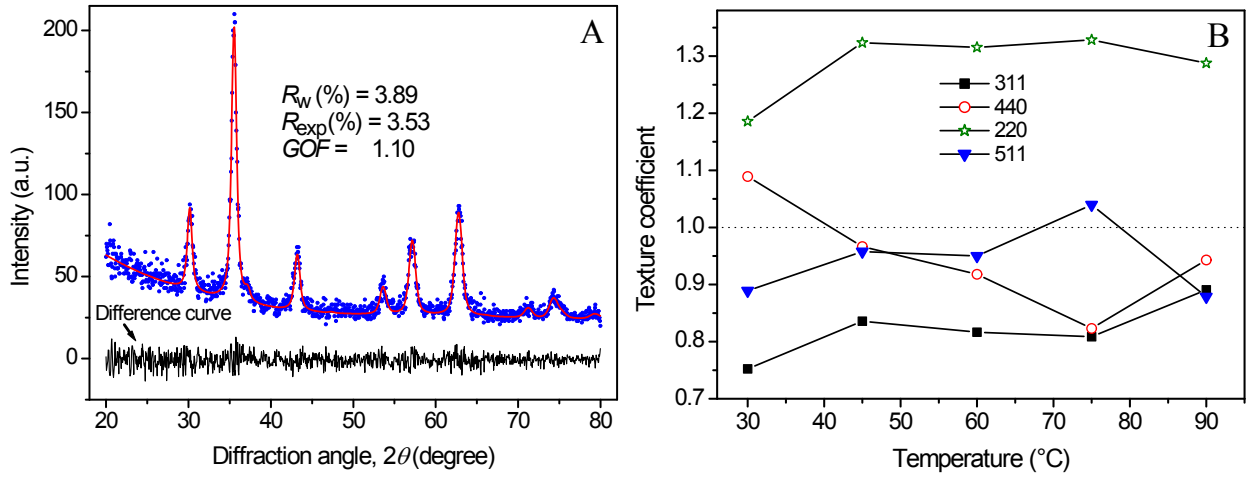

Fig. S3. (A) Rietveld refinement of X-ray powder diffraction pattern, T33 shows the composition and crystal structure of core-shell nanoparticles. (B) The texture coefficient of magnetite nanocrystals, calculated from their powder X-ray diffraction patterns (JCPDS card No. 19-0629 is used as reference for the calculations) as a function of synthesis temperature.

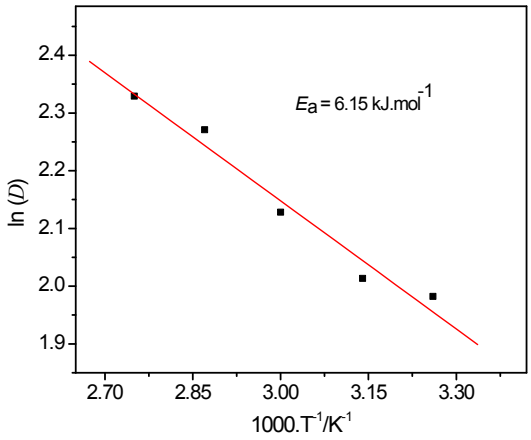

Fig. S4. Arrhenius plot of change in crystallite size as a function of reaction temperatures for ammonia precipitated magnetite samples.

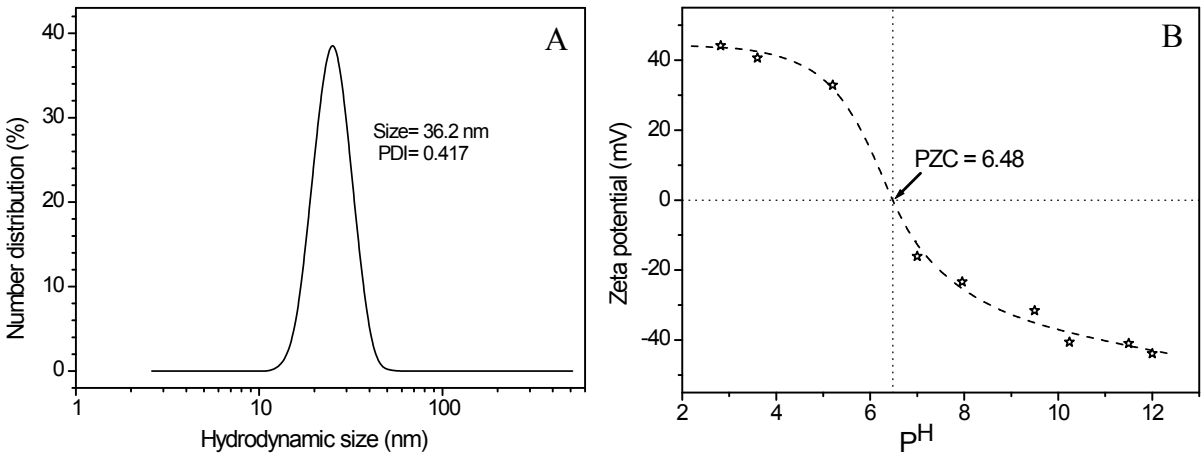

Fig. S5 (A) Particle size (hydrodynamic diameter) distribution as measured by photon scattering (number distribution) of suspensions and (B) zeta potential of T60 magnetite nanoparticles as a function of the pH.

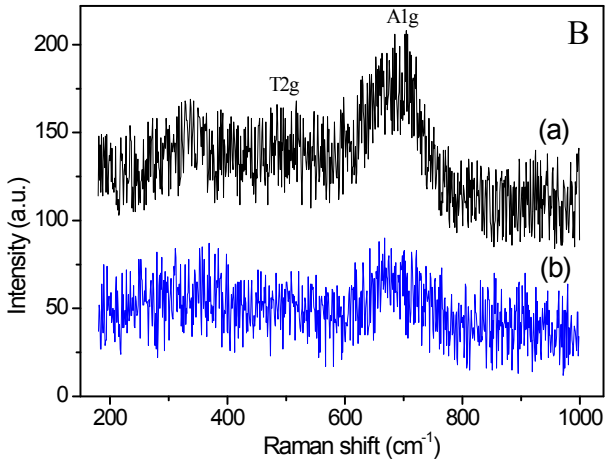

Fig. S6 Typical Raman spectra of (a) T75 and (b) T90 recorded after exposure for 60 s to 2.5 mW laser powers.

The Raman spectra taken with relatively low intensity laser power of 2.5 mW on magnetite crystals of T75 and T90 shows the co-existence of the two phases at the illuminated point. The specimen produced characteristic vibrations as broad peak at ~600 rcm^{-1} extending up to 785 rcm^{-1} which could be assigned to the A_{1g} mode, due to phonon confinement effects in the nanocrystals. A_{1g} mode is related with symmetric stretch of oxygen atoms along Fe–O bonds.[1] The peak due to the A_{1g} mode of vibration is relatively less intense in T90 and this could be due to dimensional effects or stress in the nanocrystals. The characteristic bands at 667 and 536 rcm^{-1} can be assigned to the A_{1g} and T_{2g} transitions of magnetite, respectively, which are consistent with the values reported in the literature.[2] The characteristic vibration bands belonging to magnetite can easily be distinguished from characteristic bands of γ-Fe_2O_3 at 720, 500, and 350 rcm^{-1}. Furthermore, no obvious bands of other impurities such as hematite (390, 280, 220 rcm^{-1}) or akaganeite (1110, 880 rcm^{-1}) can be detected. This further confirms that the black product is predominantly magnetite with small amount of maghemite as impurity phase.[3]

References

1 O. N. Shebanova and P. Lazor, *J. Solid State Chem.*, 2003, **174**, 424.

2 Y. S. Li, J. S. Church and A. L. Woodhead, *J. Magn. Magn. Mater.*, 2012, **324**, 1543.

3 X. F. Qu, G. T. Zhou, Q. Z. Yao and S. Q. Fu, *J. Phys. Chem. C*, 2010, **114**, 284.